Observation of magnetization reversal process for $(Sm,Ce)_2(Co, Fe, Cu, Zr)_{17}$ magnets by soft X-ray magnetic circular dichroism microscopy

Sm_2Co_{17} magnets, which have a higher saturation magnetization than $SmCo_5$, have been developed in Japan [1]. In the beginning of 1970s, the magnetic properties of Sm–Co magnets were markedly improved to more than 240 kJ/m^3 in $Sm_2(Co, Fe, Cu, Zr)_{17}$ magnets [2]. These magnets were used in small motors such as spindle motors for cassette tape players called "WALKMAN®", acoustic applications such as small speakers, microphones or pick-up sensors, and motors used in wristwatches. Sm–Co magnets contributed to the realization of unprecedent small size and light weight of electric appliances. At the beginning of 1980, Nd–Fe–B magnets were invented, replacing the Sm–Co magnets, and have been used in various applications of not only small devices but also high-power devices such as the traction motors of hybrid and electric vehicles or the compressor motors of air conditioners. However, as these markets grow, significant resource problems arise. A small portion of Nd in Nd–Fe–B was replaced with heavy rare-earth elements of dysprosium (Dy) and terbium (Tb) to achieve the high coercivity necessary to enable the use of these magnets in high-temperature and high-demagnetization-field applications. Among rare-earth elements, Dy and Tb belong to precious metals; they are mainly produced in China and their resources are limited. Even though the Sm resources are almost 1/10 of the Nd resources, Sm–Co magnets do not require Dy or Tb and have good magnetic properties at high temperature above 200°C.

It is well known that the coercivity of $Sm_2(Co, Fe, Cu, Zr)_{17}$ is determined by the magnetic domain wall motion. In the grain of this magnet, cellular structures of $Sm(Co,Cu)_5$ and $Sm_2(Co,Fe)_{17}$ phases exist, where almost 100 nm of $Sm_2(Co, Fe)_{17}$ phases is surrounded by $Sm(Co,Cu)_5$ thin platelet phases, and these $Sm_2(Co, Fe)_{17}$ phases are separated from each other. Magnetic domain walls are pinned at the phase boundary of the two phases or are in the $Sm(Co,Cu)_5$ phase. When the demagnetization field applied is greater than the pinning field, the magnetic domain wall jumps through this cellular structure and the coercivity can be determined. However, it was unclear where the initial reverse magnetic domain formed in the demagnetization process and why the rectangularity (H_k/H_{cJ}) of the demagnetization curve, where H_k is defined as the magnetic field corresponding to 90% of remanence and H_{cJ} is the coercivity, is lower than that of Nd–Fe–B sintered magnets.

We investigated the magnetization reversal process for highly aligned $Sm_{0.67}Ce_{0.33}(Co_{0.73}Fe_{0.2}Cu_{0.05}Zr_{0.02})_{7.2}$ by soft X-ray magnetic circular dichroism (XMCD) microscopy at SPring-8 **BL25SU** [3]. Figure 1(a) shows bulk demagnetization curves and Figs. 1(b–e) show the XMCD images obtained using the Co L_3 absorption edge in various magnetic fields indicated by circles in Fig. 1(a). In Figs. 1(b–e), the red (blue) region is where the magnetization is parallel (antiparallel) to the positive direction of the external magnetic field (H). White regions correspond to the neutral area in terms of magnetization or to nonmagnetic inclusions, which were identified as Sm oxide by energy dispersive X-ray spectroscopy (EDX). The magnetization saturated at +5.0 T. It was found that the initial magnetization reversal occurred at the grain boundary and in the vicinity of Sm oxide, as shown in Fig. 1(c). At –0.5 T, the reversal region extended into the grains(Fig. 1(d)), and reached the zero of magnetization i.e., coercivity (Fig. 1(e)).

Figure 2(a) is an enlargement of the area surrounded by the square in Fig. 1(d), where reversal extended into the grains at the grain boundary (Fig. 1(d)) and in the vicinity of Sm oxide (Fig. 1(e)). The local demagnetization curves for each position

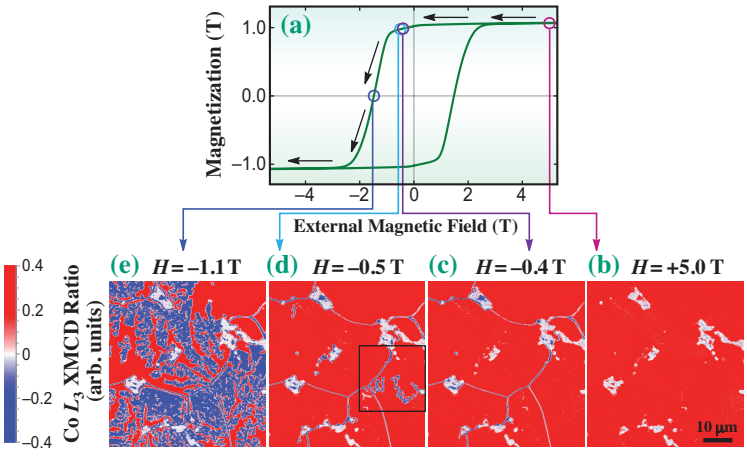

Fig. 1. Bulk demagnetization curve of anisotropic $(Sm, Ce)_2(Co, Fe, Cu, Zr)_{17}$ magnets **(a)** and XMCD images obtained using Co L_3 absorption edge under external magnetic fields of H=+5.0 T **(b)**, –0.4 T **(c)**, –0.5 T **(d)** and –1.1 T **(e)**. [3]

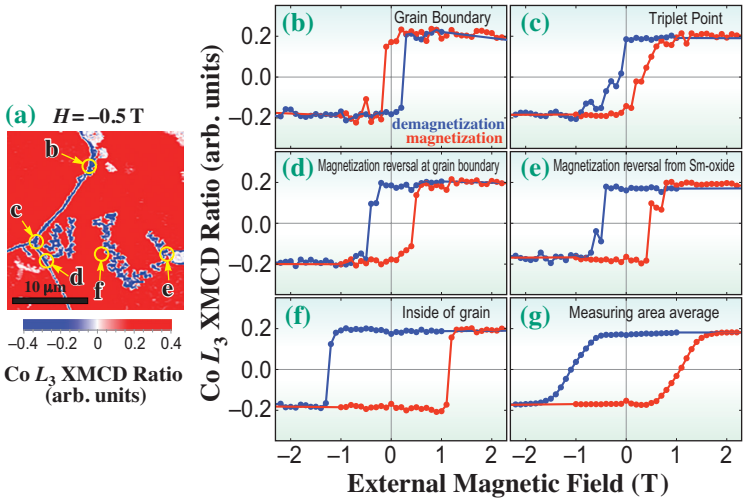

Fig. 2. Enlarged XMCD image **(a)** of the area surrounded by the square in Fig. 1(d), where initial magnetization occurred at grain boundary (b) and in the vicinity of Sm oxide, followed by magnetization reversal areas extending into grains from the grain boundary at (d) and the vicinity of Sm oxide at E in Fig. 2(a). **(b)–(f)** Local demagnetization curves at (b) to (f) marked in (a). **(g)** Average of local demagnetization curves of entire measurement area. [3]

marked by yellow circles in Fig. 2(a) are shown in Figs. 2(b–f); these were evaluated from the Co L_3-edge XMCD signal intensity. The average local demagnetization curve of the entire measurement area is shown in Fig. 2(g). It was found that the coercivity and rectangularity in local magnetic properties are different between those inside the grain (Fig. 2(f)), at the grain boundary (Fig. 2(b)), at a triplet point (Fig. 2(c)), at the starting point where a reversal domain extends into a grain (Fig. 2(d)), and in the vicinity of Sm oxide (Fig. 2(e)). It was verified that H (–0.5 T) in Fig. 2(d) agrees well with H where their magnetization starts to decrease in Fig. 2(g). To verify the composition differences between grains and the grain boundary and the vicinity of the Sm oxide, EDX line scanning was applied. Figure 3 shows the results of line scanning for Co, Fe, and Cu in the peripheral region of the grain boundary, and for Sm, Co, Fe and Cu in the vicinity of Sm oxide. At the grain boundary, it was confirmed that the amount of Fe increases and that of Cu decreases, and in the vicinity of Sm oxide, the amounts of Cu, Fe, and Co decrease and that of Sm increases.

Using the cutting-edge visualization technology of XMCD microscopy, the factors causing the deterioration of coercivity for Sm_2Co_{17} magnets were clarified and directly detected by the observation of the magnetization reversal process. The coercivities of these magnets could be increased by the improvement of the process of removing Sm oxide and by the improvement of the composition of the grain boundary.

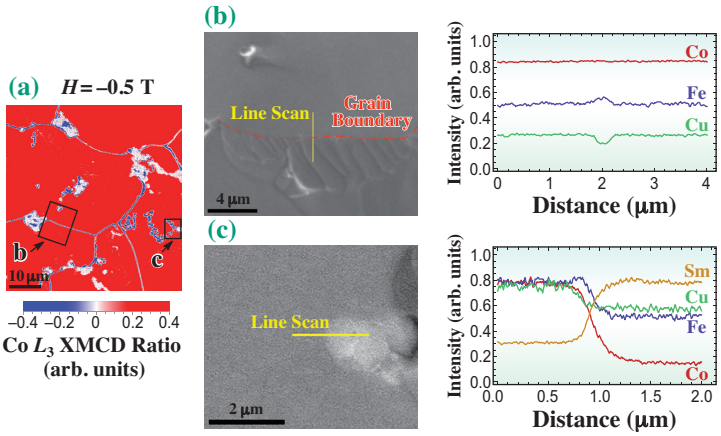

Fig.3. **(a)** Co L_3 XMCD image under external magnetic field of –0.5 T. Secondary electron microscopy images and results of line scanning at grain boundary **(b)** and in the vicinity of Sm oxide **(c)**. [3]

Y. Matsuura[a,*], R. Tamura[b], K. Ishigami[c] and T. Nakamura[c,d]

[a] Research Institute for Applied Sciences
[b] Dept. of Materials Science and Technology, Tokyo University of Science
[c] Japan Synchrotron Radiation Research Institute (JASRI)
[d] International Center for Synchrotron Rad. Innovation Smart, Tohoku University

*Email: yutaka.matsuura@rias.or.jp

References

[1] H. Senno, Y. Tawara: IEEE Trans. Magn. **10** (1974) 313.
[2] T. Ojima *et al.*: IEEE Trans. Magn. **13** (1977) 1317.
[3] Y. *Matsuura, R. Maruyama, R. Kato, R. Tamura, K. Ishigami, K. Sumitani, K. Kajiwara and T. Nakamura: Appl. Phys. Lett.* ***117*** *(2020) 022409.*